Journal of Porphyrins and Phthalocyanines
J. Porphyrins Phthalocyanines 2013; **17**: 522–528
DOI: 10.1142/S1088424613500430

Published at http://www.worldscinet.com/jpp/

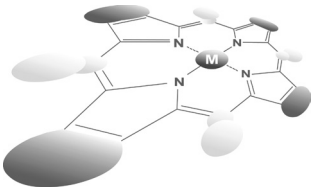

Electrochemical characterization of dilithium phthalocyanine carbonaceous electrodes

Constantin Apetrei[a,b], Cristina Medina-Plaza[a], José Antonio de Saja[c] and Maria Luz Rodriguez-Mendez*[a◊]

[a] *Department of Inorganic Chemistry, Escuela de Ingenierías Industriales, University of Valladolid, Paseo del Cauce, 59, 47011 Valladolid, Spain*
[b] *Department of Chemistry, Physics and Environment, Faculty of Sciences and Environment, "Dunarea de Jos" University of Galati, 47 Domneasca Street, 800008 Galati, Romania*
[c] *Department of Condensed Matter Physics, Faculty of Sciences, University of Valladolid, 47011 Valladolid, Spain*

Dedicated to Professor Özer Bekaroğlu on the occasion of his 80th birthday

Received 30 January 2013
Accepted 16 March 2013

ABSTRACT: Carbonaceous electrodes of dilithium phthalocyanine were prepared using graphite, carbon microspheres and multiwall carbon nanotubes. The electrochemical behavior of the dilithium bisphthalocyanine electrodes was found to be dependent on the nature of the carbonaceous material and on the nature of the electrolytic solution. The electrocatalytic properties of the dilithium phthalocyanine electrodes for oxidation of ascorbic acid were evidenced by the enhancement of the oxidation peak current, (~10 fold compared to the bare carbon electrodes) and the decrease of the oxidation potential at which oxidation of ascorbic acid takes place. The combined use of multiwall carbon nanotubes and dilithium phthalocyanine produces a synergistic effect that improves the electrocatalytic effect towards ascorbic acid.

KEYWORDS: dilithium phthalocyanine, voltammetric sensors, ascorbic acid.

INTRODUCTION

Phthalocyanines can be immobilized on inert electrode surfaces such as graphite, carbon, ITO glass, or gold and exhibit electrocatalytic activity for a variety of reactions [1–4]. These metal complexes act as mediators by lowering the overpotential of oxidation or reduction of the target molecules or increasing the intensity of the peaks observed. Therefore, phthalocyanine sensors have been applied in amperometric, voltammetric or potentiometric electrocatalytic determination of many organic and inorganic compounds.

Their catalytic action can be described in terms of chemical structure and chemical and physical properties. Their reactive centers are clearly identified and their reactivity can be modulated by changing the nature of the central metal or by modifying the structure of the macrocyclic ligand [2, 5, 6].

The number of works published using phthalocyanines as sensitive materials for electrochemical sensors is quite large and include a variety of phthalocyanine derivatives (central metal ions, substituents), electrode designs, preparation techniques and target molecules [5, 6]. Metallophthalocyanine complexes (MPc) where the phthalocyanine ring (in oxidation state -2) is coordinated to a range of transition metal ions in oxidation state +2 have been widely studied. Other families of phthalocyanines have been studied in lesser extent. For instance, some works have been dedicated to electrochemical sensors based on lanthanoid bisphthalocyanines which are sandwich type compounds with free radical character and ring oxidation state -1.5 [7–10].

The dilithium complex (Li_2Pc) is an example of a different class of phthalocyanine derivative, where the Pc

◊ SPP full member in good standing

*Correspondence to: María Luz Rodríguez-Méndez, email: mluz@eii.uva.es, tel: +34 983-423540, fax: +34 983-423310

ring is coordinated to two lithium ions [11]. Both cations cannot be accommodated in the center of the cavity and thus the lithium atoms are projected out of the plane of the phthalocyanine ring. Dilithium phthalocyanine possess mixed electronic-ionic conductivity due to overlap of π–π orbitals (electronic) and mobility of Li^+ ion (ionic) in a channel formed due to stacking of the macromolecules [12]. The electrochemical oxidation of the dilithium phthalocyanine, produces the lithium complex (LiPc) (ring oxidation state -1) that can be considered as the simplest representative of the radical phthalocyanines [11, 13–15]. As during oxidation lithium ions are liberated, these molecules have been used to prepare electrodes for solid state batteries [13]. Such electrodes have been prepared by electrodeposition [16] or by the Langmuir–Blodgett technique [12]. In spite of these interesting electrochemical and conducting properties that make dilithium phthalocyanine (Li_2Pc) a good candidate as electrode modifier, electrochemical sensors based on Li_2Pc have not been yet developed.

Electrochemical sensors based on phthalocyanines can be prepared using a variety of techniques that include, polymerization [17], sol-gel [18], Langmuir–Blodgett [4, 19] or layer by layer [20, 21] among others. One of the classical methods to prepare electrodes based on phthalocyanines is the carbon paste technique (CPE) in which the phthalocyanine is mixed with a carbonaceous material and a binder to form a paste. In addition, different types of carbonaceous materials can be used to prepare the paste [22] that include, graphite, microspheres or carbon nanotubes among others [23–25]. Microspheres have the advantage of their high specific surface and porous structure, whereas carbon nanotubes (CNT) are excellent candidates for the fabrication of electrochemical sensors because of their electrical conductivity, large surface area, low surface fouling and ability to reduce overpotentials [26–33].

In this work, carbonaceous electrodes of dilithium phthalocyanine were prepared using graphite, carbon microspheres and multiwall carbon nanotubes (MWCNT), and their electrochemical reduction/oxidation behaviors in a variety of electrolytes were studied in detail. The possibility of using the Li_2Pc as sensitive material and their electrocatalytic properties have been analyzed. The synergistic effect of MWCNT and Li_2Pc has been evaluated.

EXPERIMENTAL

All reagents, including Li_2Pc, were of high purity and used without further purification (Sigma-Aldrich). Solutions were prepared using deionized water (18.3 MΩ × cm resistivity), Milli-Q, Millipore. Carbonaceous materials used for the preparation of the CPE electrodes were: Graphite powder (High purity Ultracarbon®, Ultra F purity. Bay City, MI, USA), carbon microspheres (from Sigradur G HTW, Thierhaupten, Germany) and carbon nanotubes (multi wall nanotubes, Nanoledge Inc., Boncherville, Quebec, Canada). Carbon paste electrodes containing Li_2Pc were prepared by mixing the carbonaceous material, the dilithium phthalocyanine (15%, w/w) and Nujol (Fluka) as the binder of the composite mixture [34]. Three types of electrodes were prepared using different carbonaceous materials: graphite powder was used to prepare classical graphite based carbon paste electrodes (Li_2Pc/G-CPE), microspheres were used to prepare electrodes with high surface to volume ratio (Li_2Pc/ME-CPE) and multiwall carbon nanotubes were used to prepare electrodes that combine two electrocatalysts, Li_2Pc and MWCNT (Li_2Pc/MWCNT-CPE). Pastes were packed into the body of a 1 mL PVC (polyvinyl chloride) syringe and compressed. A metallic copper wire was used as an electrical contact. Electrochemical experiments were performed using a three electrode system with a silver/silver chloride reference electrode, a 1 cm^2 platinum counter electrode and the corresponding CPE as the working electrode. The potentiostat used was an EG&G PARC, Model 2273 potentiostat/galvanostat (Princeton Applied Research Corp.). Temperature control at 25 °C was achieved using a circulating bath (Neslab).

RESULTS AND DISCUSSION

Electrochemical studies were carried out in KCl 0.1 M. Figure 1 shows the cyclic voltammetric (CV) curves from -1.0 V to +1.0 V at 0.1 $V.s^{-1}$ for Li_2Pc carbonaceous electrodes prepared using graphite (Fig. 1a), microspheres (Fig. 1b) and nanotubes (Fig. 1c). The electrode prepared with graphite (Li_2Pc/G-CPE) shows a quasi reversible redox process at $E_{1/2}$ = -0.04 V with a peak separation (ΔE) near 0.52 V. According to literature, this redox process is assigned to phthalocyanine ring oxidation/reduction (from Pc^{2-} to Pc^{-}) that gives rise to the LiPc radical species [35]. The responses were highly stable and the electrodes could be cycled up to 100 cycles without important changes in the responses. Only a slight decrease of the intensity of the peaks was observed (about 5% for 100 cycles).

Electrodes prepared with microspheres (Li_2Pc/ME-CPE) (Fig. 1b) and nanotubes (Li_2Pc/MWCNT-CPE) (Fig. 1c) showed a similar behavior, but molecular aggregation of phthalocyanines influenced strongly the electrochemical responses. The use of carbon forms with higher active surface (as in the microspheres) caused a decrease of the separation between the anodic and the cathodic waves (ΔE = 0.504 V). This decrease was clearly more marked when using MWCNT as carbon material (ΔE = 0.426 V). This seems to indicate that the electrochemical oxidation of the Li_2Pc is facilitated in the presence of MWCNT due to the π–π interactions with the carbon nanotubes that promotes the charge transfer trough the electrode interface and/or the charge transport

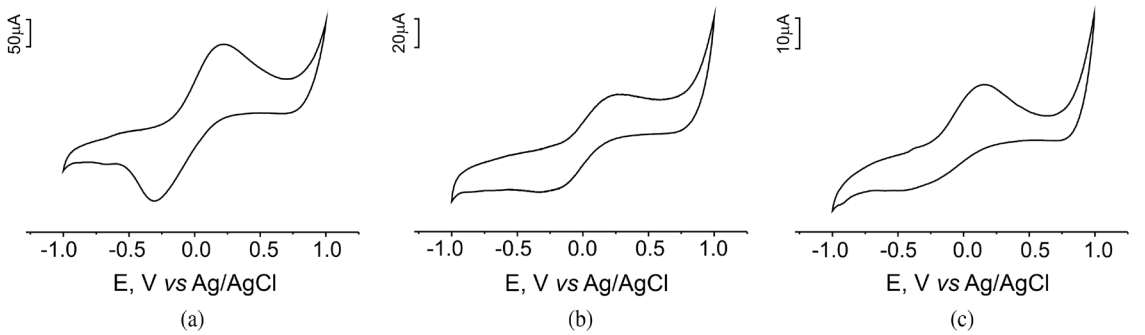

Fig. 1. Cyclic voltammograms of Li_2Pc CPE electrodes prepared using (a) graphite; (b) microspheres and (c) MWCNT as carbonaceous material recorded at a scan rate of 100 $mV.s^{-1}$ in 0.1 M KCl

within the film confirming the electrocatalytic effect of nanotubes. In contrast. MWCNT make it difficult the reduction process, probable due to the strong interaction between the nanotubes and the radical species formed upon oxidation (LiPc).

The dynamic character of the electrode process was further examined by registering voltammograms at different scan rates (Fig. 2). In all three electrodes the intensity of the peaks depends linearly with the square root of the velocity, indicating a diffusion controlled process in accordance with the Randles–Sevcik equation (Equation 1).

$$I_a = 2.687 \times 10^5 \, n^{3/2} \nu^{1/2} \, D^{1/2} \, A \, C \qquad (1)$$

where I_a is the anodic peak current (Ampere), n is the number of electrons involved in the redox process, ν is the potential scan rate ($V.s^{-1}$), D is the diffusion coefficient ($cm^2.s^{-1}$), A is the electrode surface area (cm^2), and C is the concentration (mM).

This Nerstian behavior is in good accordance with data obtained using other radical phthalocyanine-CPE sensors [23]. Table 1 shows the values of the slope of the curves obtained by representing the intensity of the anodic peaks *vs.* the square root of the scan rate. As observed in the table, the slope of the curve obtained when using MWCNT was approximately one order of magnitude higher than for the Li_2Pc/G-CPE and Li_2Pc/ME-CPE electrodes, suggesting a faster response. From the slope of I_a *vs.* $\nu^{1/2}$ plot, the diffusion coefficient D (ions diffusing inside/outside the film to maintain the electroneutrality) could be calculated (Table 1). Again, the diffusion coefficient obtained for Li_2Pc immobilized in carbon nanotubes is higher than the value obtained using other carbonaceous forms.

Table 1. Slope (m), coefficient of correlation (R^2) and diffusion coefficients (D) obtained by representing the intensity of the anodic peak and the square root of the scan rate

Electrode	m (slope)	R^2	D, $cm^2.s^{-1}$
Li_2Pc/G-CPE	4×10^{-5}	0.9606	8.94×10^{-7}
Li_2Pc/ME-CPE	3×10^{-5}	0.9936	5.03×10^{-7}
Li_2Pc/MWCNT-CPE	1×10^{-4}	0.9928	3.02×10^{-6}

It is worthily noting that although Li_2Pc/MWCNT-CPE also shows a Nerstian behavior, voltammograms registered at high scan rates appear tilted approaching progressively to an ohmic conduction. Lithium phthalocyanine (LiPc) possesses mixed electronic-ionic conductivity due to overlap of π–π orbitals (electronic)

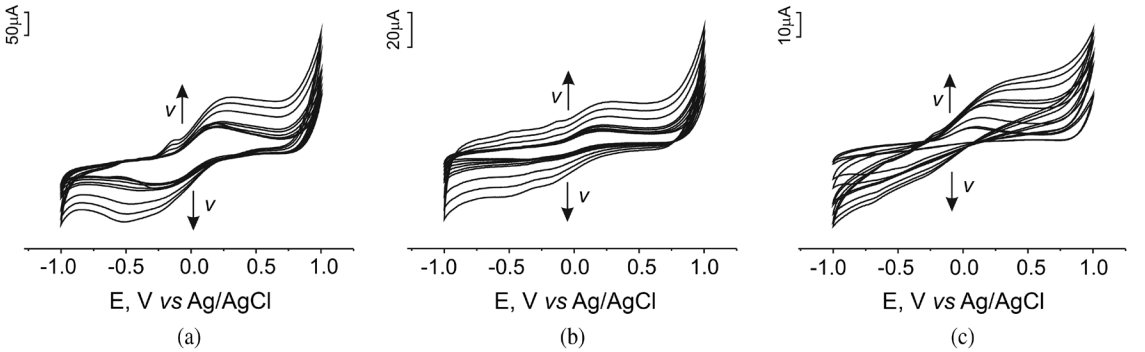

Fig. 2. Cyclic voltammograms of Li_2Pc/G-CCE (a), Li_2Pc/ME-CPE, and Li_2Pc/MWCNT-CPE (c) in 0.1 M KCl at scan rates from 50–200 $mV.s^{-1}$

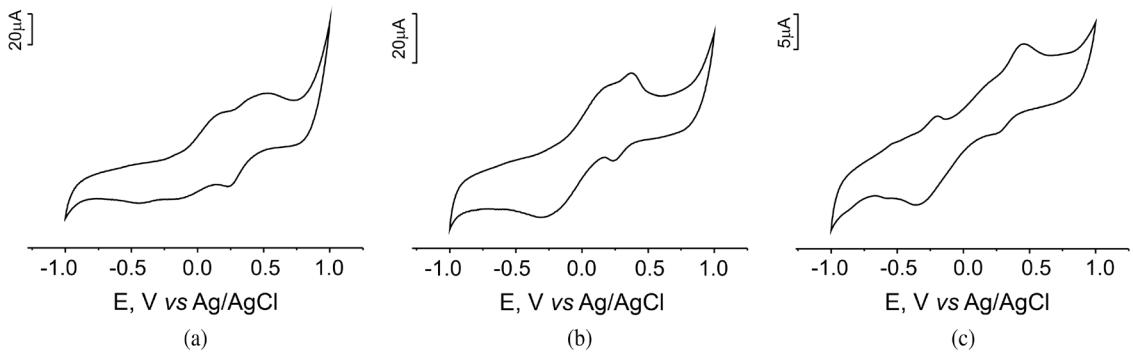

Fig. 3. Cyclic voltammograms of Li_2Pc/G-CCE (a), Li_2Pc/ME-CPE, and Li_2Pc/MWCNT-CPE (c), in 1 mM $[Fe(CN)_6]^{3-}/[Fe(CN)_6]^{4-}$ in 0.1 M KCl at 100 $mV.s^{-1}$

and mobility of Li^+ ion (ionic) in a channel formed due to stacking of the macromolecules [12]. The formation of the conductive LiPc free radical and the liberation of Li^+ ions that are trapped at the cavities of the MWCNT electrodes, can be responsible of this increase in the ohmic behavior.

Another interesting observation is that at high scan rates, the shapes of the voltammogranms registered using graphite or microspheres are different from those obtained at low scan rates and a small second peak at lower potentials is observed/anodic wave at *ca*. -0.2 V. According to the literature, this second peak could be attributed to the oxidation of Li_2Pc to the free radical of phthalocyanine H(Pc) [35]. That is, from the same starting material (the Li_2Pc), two different products can be obtained depending on the oxidation conditions. Usually, electrochemical oxidation produces the radical lithium salt (LiPc), but under certain conditions (usually chemical oxidation), the free metal HPc (where Pc is the radical anion Pc^-) can also be obtained. In our case, high scan rates could favor this new pathway.

In order to understand the electron transfer behavior of the chemically modified electrodes, we have carried out electrochemical measurements on Li_2Pc/G-CPE, Li_2Pc/ME-CPE, Li_2Pc/MWCNT-CPE in presence of ferrocyanide. The $[Fe(CN)_6]^{3-}/[Fe(CN)_6]^{4-}$ couple is used to characterize the active surface (number of active sites or blocking ability of surfaces). Results are shown in Fig. 3.

Voltammograms obtained from electrodes prepared with graphite and microspheres show two redox pairs associated with both the Li_2Pc/LiPc couple (at $E_{1/2}$ *ca*. 0.1 V) and the ferrocyanide/ferricyanide couple (at *ca*. 0.45 V). Peaks are broad and somehow overlapped. In contrast, when MWCNT are used, peaks are well separated and the peak associated with the Li_2Pc appears shifted to lower potentials (anodic wave that appears at +0.2 V in KCl shifts to -0.1 V). The most interesting feature is that the intensity of the ferrocyanide increases drastically in the presence of the MWCNT, indicating that the number of active sites is amplified. The active area calculated from voltammograms registered at different scan rates (50 to 1000 $mV.s^{-1}$) according to the Randles–Sevcik equation (taking into account that the diffusion coefficient for 10^{-3} M ferrocyanide is 7.26×10^{-6} $cm^2.s^{-1}$ in 1.0 M KCl solution) was similar for graphite and microspheres (0.157 cm^2) whereas, for the MWCNT electrode the calculated active area was 0.24 cm^2 (Table 2).

Table 2. Slope (m), and active area obtained by representing the intensity of the anodic peak and the square root of the scan rate *vs.* ferrocyanide

Electrode	m (slope)	Experimental value of active area, cm^2	Experimental value of ratio active area/ geometrical area
Li_2Pc/G-CPE	0.000155	0.19	27.273
Li_2Pc/ME-CPE	0.000114	0.157	20.059
Li_2Pc/MWCNT-CPE	0.000174	0.240	30.616

The voltammetric responses relies on the transfer of counterions between the electrolyte and the bulk of these materials in response to the electron-transfer processes associated with their oxidation and reduction. In order to evaluate the influence of the electrolyte in the electrochemical comportment, carbonaceous electrodes

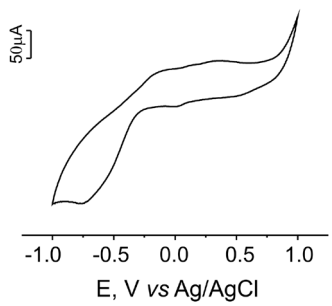

Fig. 4. Cyclic voltammogram of Li_2Pc/ME-CPE recorded at a scan rate of 100 $mV.s^{-1}$ in 0.1 M HCl

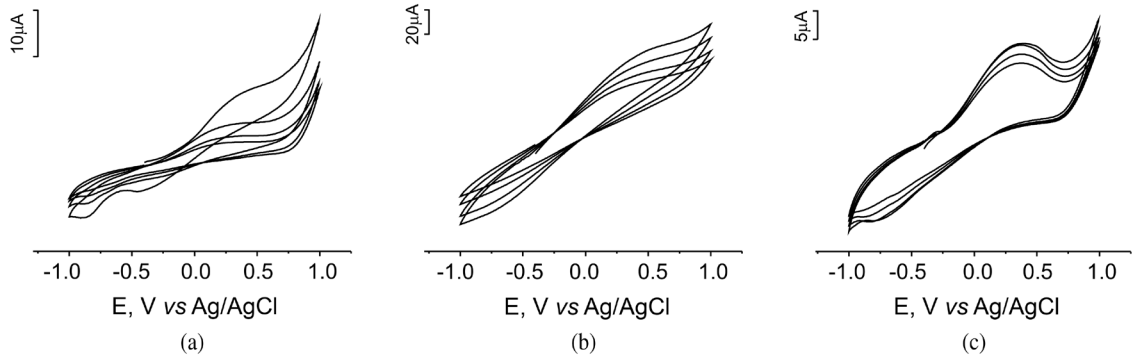

Fig. 5. Cyclic voltammograms of Li_2Pc CPE electrodes prepared using (a) graphite; (b) microspheres and (c) MWCNT as carbonaceous material recorded at a scan rate of 100 $mV.s^{-1}$ in 0.1 M $LiClO_4$

were also immersed in solutions containing different electrolytes.

The role of protons was studied by immersing the electrodes in HCl. The cyclic voltammogram of the Li_2Pc/MWCNT-CPE electrode in 0.1 mM HCl (pH = 3) is shown in Fig. 4. In the presence of protons, the three electrodes show two anodic waves of similar intensity at *ca*. -0.2 V and +0.25 V. The cathodic wave contains a small peak at +0.05 V and a broad and intense peak at -0.6 V. These two redox processes could be due to the formation of a protonated species in HCl that has also been described in other radical species [9]. This protonated ring can be oxidized at lower potentials than the neutral Li_2Pc.

As previously established, the electrochemical oxidation of the dilithium salt of phthalocyanine, the Li_2Pc, produces de monolithium radical derivative LiPc, (that possess mixed electronic-ionic conductivity) with liberation of Li^+ ions [17]. Due to the important role of Li^+ ion in the ionic conductivity of Li_2Pc, the electrochemical behavior of these electrodes was tested in a $LiClO_4$ solution. As shown in Fig. 5, the presence of Li^+ ions produces two effects in the CVs. The first effect is an increase in the separation between the anodic and cathodic waves of the redox pair Li_2Pc/LiPc while voltammograms become tilted and show an increased ohmic behavior. This may be the result of an increase in their conductivity through the easier transfer of the Li^+ ions in the presence of lithium in the solution. In addition, the IR drop for electrolyte motion in carbon pores affects the double-layer formation mechanism, in which the charge stored is recognized to be distributed. The second effect is that the intensity of the peaks decreases upon successive cycling, indicating that the active sites are progressively blocked. This decrease is dependent on the surface area of the carbonaceous materials and follows the trend Li_2Pc/G-CPE > Li_2Pc/ME-CPE > Li_2Pc/MWCNT-CPE. That is, in MWCNT this effect is almost negligible.

When using NH_4OH as electrolyte, the responses are highly similar to those obtained in $LiClO_4$. The cyclic voltammograms also become tilted and pointed at each end and the intensity changes almost linearly with potential over a very wide range (Fig. 6). But in this case, all modified electrodes showed improved stability and the blocking effect is almost unexistent. These results indicate that NH_4^+ ions can also participate in the ions motion inside the electrodes and to the double layer formation, but the basic environment prevents the blocking of the active sites.

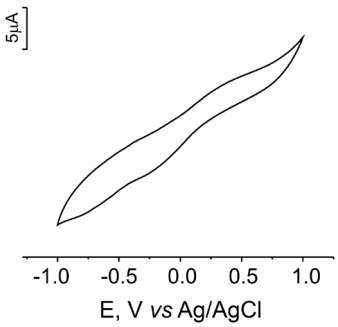

Fig. 6. Cyclic voltammogram of Li_2Pc/ME-CPE electrodes recorded at a scan rate of 100 $mV.s^{-1}$ in 0.1 M NH_4OH

Finally, the response of the electrodes towards an antioxidant of interest in the food industry such as the ascorbic acid was tested (Fig. 7). Voltammograms show peaks of two different origins: peaks associated with the oxidation-reduction of the ascorbic acid present in the solution and transient responses associated with the electrode material (Li_2Pc). But, the important issue is that the interactions that occur between the electrode and the ascorbic acid can improve the electrochemical signals.

In all three electrodes, the electrocatalytic behavior of Li_2Pc causes a decrease in the oxidation potential of the ascorbic acid that using a bare electrode appears at 0.62 V, but shifts to lower potentials in the presence of Li_2Pc (0.57 V in Li_2Pc/G-CPE, 0.50 V in Li_2Pc/ME-CPE and 0.45 V in Li_2Pc/MWCNT-CPE). In addition, the anodic peak associated with the Li_2Pc also appears at lower potentials (-0.07 V).

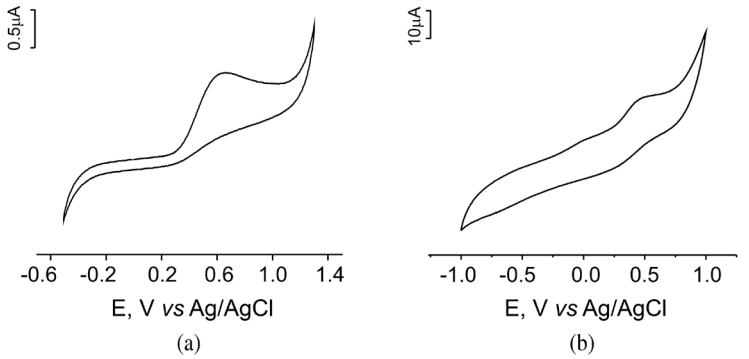

Fig. 7. Cyclic voltammograms of (a) bare MWCNT-CPE and (b) Li_2Pc/MWCNT-CPE electrodes recorded at a scan rate of 100 $mV.s^{-1}$ in 0.4×10^{-4} M ascorbic acid

Catalysis was also evidenced by the enhancement of the oxidation peak current, (~10 fold compared to the bare MWCNT electrodes). The charge passed under the curve was larger for MWCNT than for microspheres or graphite. This result indicates that carbon nanotubes facilitate the charge transfer trough the electrode interface and/or the charge transport within the film. The strong electrocatalytic effect observed in the Li_2Pc/MWCNT-CPE immersed in ascorbic acid can be attributed to the synergistic effect between MWCNT and Li_2Pc that improves electrocatalysis for the detection of ascorbic acid. This is illustrated in Fig. 7 where the response of a bare MWCNT-CPE and a Li_2Pc/MWCNT-CPE towards ascorbic acid is shown.

CONCLUSION

The electrochemical behaviour of carbonaceous electrodes of dilithium phthalocyanine prepared using graphite, carbon microspheres and multiwall carbon nanotubes, has been analyzed. The three carbon materials are adequate for the immobilization of Li_2Pc and show distinct electrochemical behaviours that are related to the nature of the carbon material. The electrode formed by combining MWCNT and the Li_2Pc shows a higher diffusion coefficient and an increased number of active sites. The electrochemical response registered in different electrolytic solutions was found to be largely dependent on the nature of the ions present in the solution. In the presence of protons, the electrodes showed two anodic waves produced by the protonation of the Pc ring, whereas the presence of $LiClO_4$ or NH_4OH, the mobility of lithium ions is promoted increasing the ohmic conduction. The electrodes were also used to detect citric acid, an antioxidant of interest in the food industry. It was demonstrated that the electrocatalytic properties of the Li_2Pc facilitate the oxidation of the citric acid. The simultaneous use of two electrocatalysts MWCNT and Li_2Pc produced a synergic effect that improved the electrocatalytic effect.

Acknowledgements

Financial support of the CICYT Spanish Ministry of Science (Grant AGL2012-33535) is gratefully acknowledged. One of us, CMP wants to thank the University of Valladolid for a PhD Grant (PIF-UVa).

REFERENCES

1. Jiang J. *Functional Phthalocyanine Molecular Materials*. *Series: Structure and Bonding 135, 1st Ed.*, Springer: 2010.
2. Zagal JH, Griveau S, Silva JF, Nyokong T and Bedioui F. *Coord. Chem. Rev.* 2010; **254**: 2755–2791.
3. Rodríguez-Méndez ML. In *Sensing Properties of Phthalocyanines in Encyclopedia of Sensors*, Vol. 9, Grimes CA, Dickey EC and Pishko MV. (Eds.) American Scientific Publishers: California, USA, 2006; pp 111–134.
4. Valli L. *Adv. Col. Interf. Sci.* 2005; **116**: 13–44.
5. Lever ABP. *J. Porphyrins Phthalocyanines* 1999; **3**: 488–499.
6. Bedioui F, Griveau S, Nyokong T, Appleby AJ, Caro CA, Gulppi M, Ochoa G and Zagal JH. *Phys. Chem. Chem. Phys.* 2007; **9**: 3383–3396.
7. Weiss R and Fischer J. In *Lanthanide Phthalocyanine Complexes, The Porphyrin Handbook*, Vol. 16, Kadish KM, Smith KM and Guilard R. (Eds.) Academic Press: New York, 2003; pp 171–246.
8. Rodríguez-Méndez ML, Gay M and de Saja JA. *J. Porphyrins Phthalocyanines* 2009; **13**: 1159–1167.
9. Gay M, Muñoz R, de Saja JA and Rodriguez-Mendez ML. *Electrochim. Acta* 2012; **68**: 88–94.
10. Parra V, Hernando T, Rodríguez-Méndez ML and de Saja JA. *Electrochim. Acta* 2004; **49**: 5177–5185.
11. Bouvet M. In *Radical Phthalocyanines and Intrinsic Semiconduction, The Porphyrin Handbook*, Vol. 19, Kadish KM, Smith KM and Guilard R. (Eds.) Academic Press: New York, 2003; pp 37–104.

12. Xiang HQ, Tanaka K, Takahara A and Kajiyama T. *Langmuir* 2002; **18**: 2223–2228.
13. Scanlon LG, Lucente LR, Feld WA, Sandi G, Balbuena PB, Alonso PR and Turner A. J. *Electrochem. Soc.* 2004; **151**: A1338–A1343.
14. Deng X, Porter III WW and Vaid TP. *Polyhedron* 2005; **24**: 3004–3011.
15. Turek P, Petit P, Andre JJ, Simon J, Even R, Boudjema B, Guillaud G and Maitrot M. *J. Am. Chem. Soc.* 1987; **109**: 5119–5122.
16. Ilangovan G, Zweier JL and Kuppusamy P. *J. Physical Chemistry* 2000; **104**: 4047–4059.
17. Griveau S, Gulppi M, Pavez J, Zagal JH and Bedioui F. *Electroanalysis* 2003; **15**: 779–785.
18. Guo Y and Guadalupe AR. *Sens. Actuators B* 1998; **46**: 213–219.
19. Gorbunova Y, Rodríguez-Méndez ML, Kalashnikova IP, Tomilova L and de Saja JA. *Langmuir* 2001; **17**: 5004–5010.
20. Demel J and Lang K. *Eur. J. Inorg. Chem.* 2012; **32**: 5154–5164.
21. Volpati D, Alessio P, Zanfolim AA, Storti FC, Job AE, Ferreira M, Riul Jr. A, Oliveira Jr. ON and Constantino CJL. *J. Physical Chemistry B* 2008; **112**: 15275–15282.
22. Svancara I, Vytras K, Barek J and Zima J. *Crit. Rev. Anal. Chem.* 2001; **31**: 311–345.
23. Apetrei C, Apetrei IM, de Saja JA and Rodriguez-Méndez ML. *Sensors* 2011; **11**: 1328–1344.
24. Ruiz-Morales JC, Canales-Vázquez J, Marrero-López D, Savvin SN, Nunez P, Dos Santos-García AJ, Sánchez-Bautista C and Peña-Martínez J. *Carbon.* 2010; **48**: 3964–3967.
25. Jacobs CB, Peairs MJ and Venton BJ. *Anal. Chim. Acta* 2010; **662**: 105–127.
26. Mamuru SA, Ozoemena KI, Fukuda T, Kobayashi N and Nyokong T. *Electrochim. Acta* 2010; **55**: 6367–6375.
27. Chen Y, Lin Y, Liu Y, Doyle J, He N, Zhuang XD, Bai JR and Blau WJ. *J. Nanosci. Nanotech.* 2007; **7**: 1268–1283.
28. Bandaru PR. *J. Nanosci. Nanotech.* 2007; **7**: 1239–1267.
29. Inagaki M, Kaneko K and Nishizawa T. *Carbon* 2004; **42**: 1401–1417.
30. Zagal JH, Griveau S, Ozoemena K, Nyokong T and Bedioui F. *J. Nanosci Nanotech.* 2009; **9**: 2201–2214.
31. Ozoemena KI, Nyokong T, Knosi D, Chambrier I and Cook MJ. *Electrochim. Acta* 2007; **52**: 4132–4143.
32. Apetrei C, Nieto M, Rodríguez-Méndez ML and de Saja JA. *J. Porphyrins Phthalocyanines* 2011; **15**: 908–917.
33. Khene S and Nyokong T. *Electroanalysis* 2011; **23**: 1901–1911.
34. Rodríguez-Méndez ML, Gay M, Apetrei C and De Saja JA. *Electrochim. Acta* 2009; **54**: 7033–7041.
35. Sugimoto H, Higashi T and Mori M. *J. Chem. Soc., Chem. Commun.* 1983; **11**: 622–623.

